ENHANCING THE MECHANICAL PROPERTIES OF COMMERCIAL ALUMINUM ALLOY AA6061 BY FORWARD EXTRUSION COMBINED WITH T6 HEAT TREATMENT

NÂNG CAO ĐẶC TÍNH CƠ HỌC CỦA HỢP KIM NHÔM THƯƠNG MẠI AA6061 BẰNG ÉP CHẢY XUÔI KẾT HỢP VỚI XỬ LÝ NHIỆT T6

Lai Dang Giang, Nguyen Manh Tien*

Le Quy Don Technical University, Vietnam

*Corresponding author: manhtiennguyen84@lqdtu.edu.vn

(Received: February 03, 2026; Revised: May 06, 2026; Accepted: May 20, 2026)

DOI: 10.31130/ud-jst.2026.24(5A).082E

Abstract - This study examines the improvement of mechanical properties of AA6061 aluminum alloy by combining forward extrusion and T6 heat treatment. Finite element modeling (FEM) using Deform 3D identified three deformation stages, with a maximum extrusion load of about 14.3 tons, and experiments confirmed the feasibility of the designed die and produced sound preforms. After extrusion, specimens were solution-treated at 540°C for 2 h and artificially aged at 160–180°C for 6–18 h. Mechanical tests showed marked enhancements compared with the annealed condition. The ultimate tensile strength (UTS) of 360 MPa was achieved at 175°C for 8 h, corresponding to an increase of approximately 70%, while microhardness increased by 52.3%. Elongation (EL) was maintained at an acceptable level of about 14–20%. These results demonstrate that the proposed process effectively enhances the mechanical performance of AA6061 for lightweight structural applications.

Key words - Aluminum alloy AA6061; forward extrusion; T6 heat treatment; finite element modeling (FEM); mechanical properties

Tóm tắt - Nghiên cứu này đánh giá sự cải thiện tính chất cơ học của hợp kim nhôm AA6061 thông qua sự kết hợp giữa ép chảy xuôi và xử lý nhiệt T6. Mô hình phần tử hữu hạn bằng Deform 3D đã xác định ba giai đoạn biến dạng, với lực ép đùn cực đại khoảng 14,3 tấn; các thí nghiệm thực tế xác nhận tính khả thi của bộ khuôn và tạo ra phôi đạt yêu cầu. Sau ép chảy, các mẫu được tôi ở 540°C trong 2 giờ và hóa già nhân tạo ở 160–180°C trong 6–18 giờ. Kết quả thử nghiệm cơ tính cho thấy sự cải thiện rõ rệt so với trạng thái ủ. Giới hạn bền kéo lớn nhất đạt 360 MPa tại 175°C trong 8 giờ, tăng khoảng 70%, trong khi độ cứng tế vi tăng 52,3%. Độ giãn dài vẫn được duy trì ở mức chấp nhận được (14–20%). Những kết quả này chứng minh hiệu quả của phương pháp đề xuất cho các kết cấu nhẹ, độ bền cao.

Từ khóa - Hợp kim nhôm AA6061; ép chảy xuôi; xử lý nhiệt T6; mô hình phần tử hữu hạn (FEM); đặc tính cơ học

1. Đặt vấn đề

Aluminum alloys have long been recognized as essential engineering materials owing to their favorable combination of low density, corrosion resistance, formability, and moderate strength. Among these, the heat-treatable 6xxx series alloys, particularly AA6061, are extensively employed in automotive, aerospace, marine, and structural applications. Their widespread utilization is attributed to an attractive balance between cost, mechanical performance, and manufacturability [1 - 3]. Nevertheless, the as-cast or annealed states of AA6061 typically exhibit relatively low strength levels, which restrict their use in high-performance load-bearing components. To achieve the demanding requirements of modern lightweight structures, the mechanical properties of this alloy must be substantially enhanced through thermomechanical processing and heat treatment routes [4].

A conventional approach to strengthening aluminum alloys involves a combination of plastic deformation and subsequent precipitation hardening. Extrusion is a widely adopted forming process for aluminum alloys because it not only provides the desired product geometry but also induces significant plastic deformation that alters the microstructure. In particular, forward extrusion has the advantages of high productivity, dimensional accuracy, and the ability to process long products with controlled surface quality [5, 6]. During extrusion, intense shear and compressive stresses promote the breakdown of coarse grains and the development of elongated substructures. This deformation-induced refinement increases dislocation density and accelerates subsequent precipitation kinetics during aging treatments. At the same time, extrusion improves defect closure and homogenizes the material, thereby enhancing both mechanical properties and service reliability [7].

The heat-treatable nature of AA6061 alloy further allows it to undergo precipitation hardening, with the T6 temper being one of the most effective routes. The T6 heat treatment typically involves three stages: solution treatment, rapid quenching, and artificial aging at intermediate temperatures. In the solution treatment stage, soluble phases such as Mg_2Si are dissolved into a supersaturated solid solution. Rapid quenching retains this supersaturation by suppressing immediate precipitation. Subsequent artificial aging promotes the controlled nucleation and growth of fine, coherent precipitates, which serve as effective obstacles to dislocation motion. The resulting microstructure is characterized by a dispersion of strengthening phases that significantly raise yield strength, ultimate tensile strength, and microhardness [8, 9]. However, the treatment parameters, including solution temperature, soaking time, and aging conditions, must be carefully optimized to balance strength and ductility [10].

Numerous studies have demonstrated the efficacy of T6 heat treatment in improving the performance of AA6061 and related alloys in various conditions. Investigations on welded joints, cast products, and rolled sheets have consistently reported substantial increases in tensile strength and microhardness following T6 tempering [11, 12].

The improvements are generally attributed to microstructural refinement and precipitation hardening. However, most of these works focus on either the standalone effect of heat treatment or the mechanical response of welded and cast structures. Research that systematically integrates deformation processing, particularly extrusion, with heat treatment has received comparatively less attention. However, the combined effect of deformation-induced microstructural modification and subsequent precipitation hardening is well recognized as an effective approach to enhance the overall performance of the alloy [13].

Forward extrusion, when combined with T6 heat treatment, is expected to offer several advantages. First, the extrusion process creates a refined and defect-minimized microstructure, providing a favorable starting point for precipitation reactions. Second, the strain introduced during extrusion enhances vacancy concentration and dislocation density, which can serve as preferential nucleation sites for precipitates during artificial aging. Third, the geometry achieved by extrusion allows the production of near-net-shape components, thereby reducing material waste and improving production efficiency. When followed by T6 tempering, the alloy can simultaneously benefit from deformation hardening and precipitation strengthening, leading to superior mechanical performance while retaining acceptable ductility [14].

Finite element simulation tools, such as DEFORM-3D, have further enabled researchers to analyze extrusion processes with higher accuracy. By modeling stress–strain distribution, temperature fields, and load requirements, these simulations provide insights into the material flow during extrusion and help optimize die design and process parameters. Numerical modeling also allows a predictive evaluation of extrusion load and deformation zones, which is crucial for verifying the feasibility of experimental trials and scaling up to industrial production [15].

In this study, a finite element modeling approach using Deform-3D is employed to analyze the deformation behavior and extrusion force during forward extrusion of AA6061, guiding the subsequent experimental design. Simulation-guided extrusion experiments combined with T6 heat treatment are then conducted, followed by mechanical testing to evaluate the resulting properties. Although extrusion and T6 heat treatment have been individually applied to AA6061 alloy, the present work emphasizes their synergistic interaction, in which pre-deformation induced by forward extrusion modifies the defect structure and accelerates precipitation kinetics during subsequent aging. Unlike conventional T6 treatment applied to undeformed material, the proposed processing route achieves comparable or superior strength levels within shorter aging times, thereby improving overall processing efficiency. Furthermore, the combined numerical–experimental framework provides a practical reference for extrusion parameter selection and heat treatment optimization in industrial applications. In this work, the FEM simulation serves as a practical tool to guide experimental design by providing key insights into deformation behavior, extrusion force, and process parameters, thereby supporting die design and reducing trial-and-error.

2. Materials and methods

In this study, a commercial AA6061 aluminum alloy was used as the research material. This alloy belongs to the Al–Mg–Si system and is heat-treatable, widely applied in aerospace, automotive, and structural components due to its balanced mechanical properties and corrosion resistance. The nominal chemical composition of the alloy, determined by optical emission spectroscopy, is as follows (in wt.%): Mg 0.92, Si 0.65, Cu 0.25, Cr 0.15, Fe 0.35, Mn 0.05, Zn 0.02, Ti 0.02, with the remainder being Al. The material was supplied in the annealed condition to ensure a homogeneous microstructure and minimize residual stress.

To predict the deformation behavior of the alloy during cold forward extrusion, numerical simulations were carried out using DEFORM-3D software. The constitutive behavior of the AA6061 alloy during deformation was described using the Ludwik strain-hardening model, which is widely used to represent plastic deformation of metallic materials under cold forming conditions. The model is expressed as: $\sigma=k.\varepsilon^n$, where σ is the flow stress (MPa), ε is the true plastic strain, K is the strength coefficient, and n is the strain-hardening exponent. The material parameters were determined from uniaxial tensile tests. Tensile specimens were machined from AA6061 strips and tested on an MTS universal testing machine at a crosshead speed of 2 mm/min (Figure 1a). The stress–elongation curves were recorded automatically (Figure 1b,c), from which the values of K = 202 MPa and n = 0.175 were obtained. It should be noted that the Ludwik model is based on uniaxial stress conditions and assumes that material behavior is governed primarily by strain hardening, while the effects of strain rate sensitivity and deformation-induced temperature rise are neglected. Therefore, it represents an approximation when applied to the triaxial stress state encountered during forward extrusion. Nevertheless, since the extrusion process in this study was conducted under cold conditions with moderate forming speeds, these effects are considered limited. Under such conditions, simplified constitutive models have been reported to provide reasonable predictions of extrusion load and stress distribution. Therefore, the present model is considered adequate for qualitative analysis of deformation stages and for preliminary die and process design. This constitutive model was subsequently implemented in the DEFORM-3D software to simulate the extrusion process (Figure 1d).

The extrusion process was assumed to be carried out under cold conditions at room temperature. The temperature rise due to plastic deformation was not explicitly considered in the simulation. This assumption is reasonable for the present study, as the forming process was conducted at moderate speeds, where deformation-induced heating is expected to be limited. Therefore, its influence on the predicted extrusion load and deformation behavior is considered negligible.

In the geometric model, the billet was assumed to be an elasto-plastic deformable body, while the punch and die were considered rigid (Figure 1e). In the numerical simulations, the ram speed was set to three levels corresponding to slow (v = 5 mm/s), medium (v = 15 mm/s), and high speed (v = 30 mm/s) conditions. The contact friction coefficients were determined to be 0.08, 0.10, and 0.12, corresponding to zinc sulfate powder, synthetic oil, and mineral oil lubricants, respectively. The die fillet radii used in the simulations were set to 1 mm, 2 mm, 3 mm, and 4 mm [20, 21]. The simulation results identified three characteristic stages of the extrusion process, and provided the distributions of stress and strain within the billet. Additionally, the effects of the processing parameters and tooling conditions on the deformation of the billet were analyzed to support the experimental procedure.

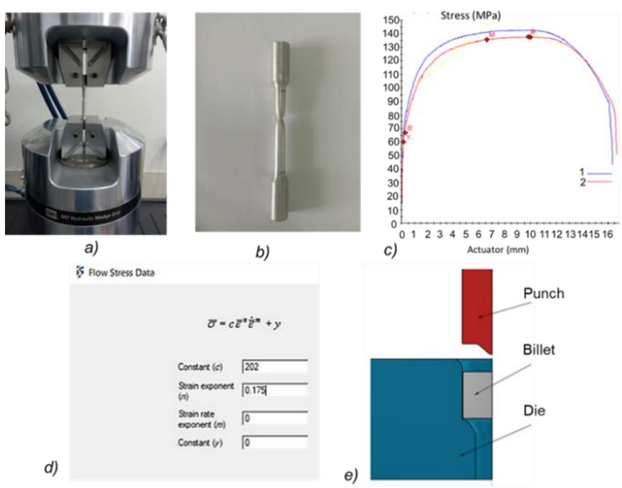

Figure 1. *Development of the constitutive model for the AA6061 alloy*

Cylindrical billets with a diameter of 21 mm and a length of 15 mm were machined from the as-received stock, and the outer oxide layer was removed by turning to achieve the required dimensional accuracy and surface quality for extrusion (Figure 2a).

Forward extrusion experiments were performed on the YHQ-SF150 hydraulic press equipped with a die made of SKD61 tool steel, chosen for its high thermal and wear resistance (Figure 2b and Figure 2c). A lubricant mixture of oil and graphite was applied to reduce friction and prevent sticking. During extrusion, the punch load was continuously recorded using a load cell attached to the press. Post-extrusion, the specimens were subjected to T6 heat treatment, consisting of solutionizing at 540°C ± 5 °C for 2 h, water quenching at room temperature. After quenching, the specimens were transferred to the aging furnace as quickly as possible to minimize the effect of natural aging at room temperature. Artificial aging was carried out to promote the formation of fine, stable precipitates uniformly distributed within the aluminum matrix, thereby enhancing the mechanical properties and achieving the required performance of the product.

The aging process for AA6061 alloy in the T6 condition is typically conducted at temperatures ranging from 160°C to 180°C for holding times of 6 h to 18 h. Aging was performed at 160 ± 2°C for aging times of 6 h, 12 h, and 18 h. According to [16, 17], the conventional T6 temper for AA6061 aluminum alloy typically employs aging at 160°C for about 18 h. Aging was conducted at 175 ± 2°C for 6 h, 8 h, and 10 h, where aging at 175°C for 8 h provides optimal strengthening. Aging was carried out at 180 ± 2°C for 4 h, 6 h, and 8 h. Although higher aging temperatures can shorten the required aging time and improve process efficiency, care must be taken to avoid over-aging, which may result in precipitate coarsening and property degradation [18, 22, 23]. The T6 heat treatment conditions applied after forward extrusion are detailed in Table 1. Specimen No. 1 corresponds to the sample after forward extrusion, while specimen No. 2 represents the sample after solution treatment. Specimens No. 3–11 correspond to the samples after the aging process.

Figure 2. *Initial billet (a), hydraulic press (b), and forward extrusion die (c)*

Table 1. *T6 heat treatment conditions are applied after forward extrusion*

Number of billets	Solution treatment (°C/h)	Aging temperature (°C)	Aging time (h)	Cooling method
No. 1	-	-	-	-
No. 2	540/2	-	-	Water quenching
No. 3	540/2	160	6	Water quenching
No. 4			12	
No. 5			18	
No. 6	540/2	175	6	Water quenching
No. 7			8	
No. 8			10	
No. 9	540/2	180	4	Water quenching
No. 10			6	
No. 11			8	

The mechanical properties of the processed specimens were evaluated to verify the effectiveness of the combined forward extrusion and T6 heat treatment. Tensile specimens were prepared in accordance with the ASTM E8/E8M standard, with a gauge length of 15 mm and a diameter of 3 mm. The tensile tests were conducted using a Devotrans universal testing machine at a crosshead speed of 1 mm/min to determine the UTS, and EL. Microhardness measurements were performed using a Wilson Wolpert Vickers microhardness tester to assess the surface microhardness of the specimens. The experimental results were compared with numerical simulations to provide a comprehensive assessment of the effects of forward extrusion and T6 heat treatment on the mechanical behavior of the AA6061 alloy. For each experimental condition, at least three specimens were tested to ensure the reliability of the results. The reported values represent the average of these measurements. The variation among the repeated tests was within an acceptable range (approximately ±5%), indicating good repeatability. For clarity, only the average values are presented in this study.

3. Results and discussion

3.1. Evaluation of numerical simulation results

The variation in the stress field of the billet during the extrusion process can be divided into several stages. Stage 1: As the punch descends and makes contact with the billet, the cold upsetting stage initiates. At the initial stage, when the punch comes into contact with the billet, the applied load is not yet sufficient to cause plastic deformation, and the material primarily undergoes elastic deformation. Only the portion of the billet in contact with the working surface of the punch, where the contact area is small, begins to experience localized plastic deformation under the applied load.

As shown in Figure 3a, the region of the billet in contact with the punch exhibits an equivalent stress of approximately 156 MPa, indicating that plastic deformation occurs rapidly at the protruding contour of the punch tip. The remaining regions, where the equivalent stress is below 93 MPa, still undergo elastic deformation. This observation is consistent with the theoretical expectation for AA6061-O aluminum alloy, which has a yield stress of approximately 110 MPa. As the punch continues to move downward, plastic deformation progresses at the concave region of the billet. In this central zone, the equivalent stress reaches about 140 MPa, while the surrounding areas, exhibiting stresses around 108 MPa, begin to transition from elastic to plastic deformation. During this stage, the cold upsetting process takes place, as illustrated in Figure 3b. The remaining regions exhibit equivalent stresses below 124 MPa and are still undergoing elastic deformation, as the metal begins to strain harden, leading to an increase in flow stress. This process occurs when the billet material starts to flow into the die cavity during extrusion. Stage 2: The upsetting process ends, and the metal begins to flow through the die cavity, marking the start of the forward extrusion process. At this stage, the metal starts to flow into the die cavity, the cold upsetting process is completed, and forward extrusion takes place (Figure 4a). The stress in most regions of the billet reaches values above 124 MPa, while the portion of the billet in contact with the die's fillet radius begins to deform under a stress of approximately 170 MPa. At the end of this stage, the metal completely fills the die cavity, and the stress within this region exceeds 187 MPa (Figure 4b). In this zone, the material is subjected to triaxial compressive stress, while the billet is simultaneously drawn in the punch's compression direction, resulting in pronounced strain hardening. For the AA6061 aluminum alloy, strain hardening intensifies with increasing deformation, leading to a corresponding rise in flow stress.

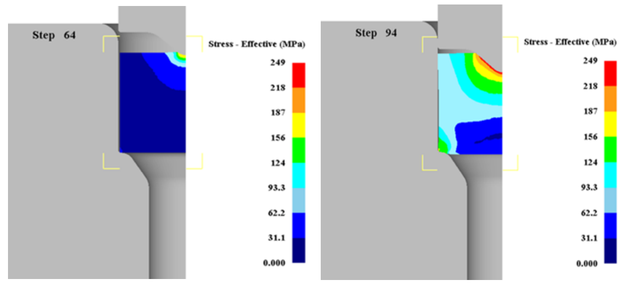

a) *b)*

Figure 3. *Stage 1 of the forward extrusion process for the AA6061 billet*

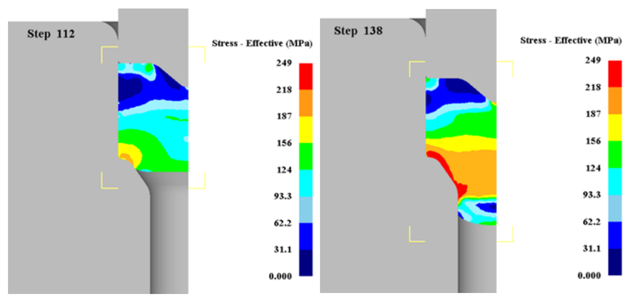

a) *b)*

Figure 4. *Distribution of the stress field during stage 2 of the forward extrusion process*

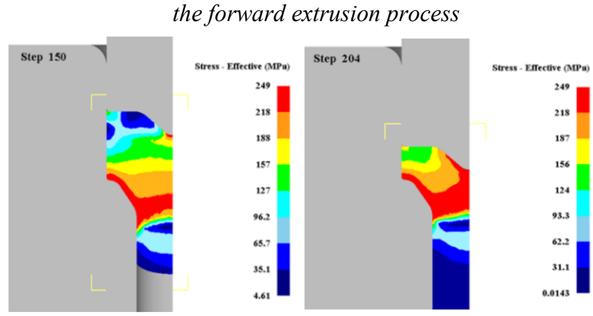

a) *b)*

Figure 5. *Distribution of the stress field during stage 3 of the forward extrusion process*

The forward extrusion process proceeds intensively until the desired product dimensions are achieved, marking the end of the extrusion process (Stage 3). As the punch continues to move downward, the metal flows within the die cavity in the direction of the punch, with the maximum stress exceeding 218 MPa at the die's fillet radius and the central region of the billet (Figure 5a). Due to the strain-hardening phenomenon in the AA6061 alloy, the maximum equivalent stress in the material (249 MPa) increases by approximately 78% compared to the tensile strength of the annealed AA6061 alloy (140 MPa). During this stage, the stress remains high and stable until the extrusion process is completed. Therefore, this stage exhibits greater stability compared to the previous stages. The punch continues to move downward, pushing the metal until the product reaches the desired dimensions, at which point the punch stops, and the extrusion process concludes (Figure 5b). Thus, the stress in the billet gradually increases through each stage, reaching its highest and most stable value in the final stage.

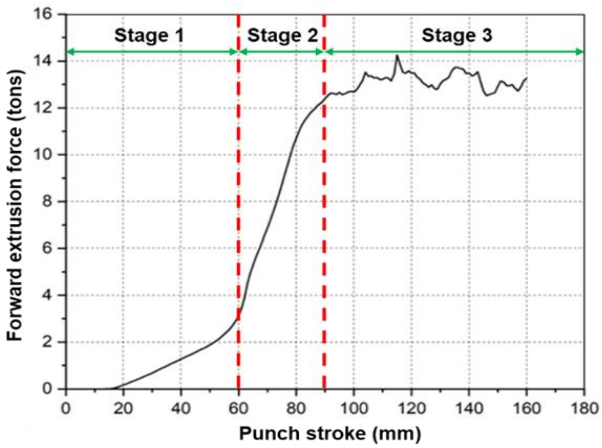

Figure 6. *Forward extrusion force diagram simulated using Deform 3D software*

As shown in Figure 6, the force during the forward extrusion process can be divided into three distinct stages. Stage 1 corresponds to the breakdown of the crystal lattice structure, during which the upsetting (cold upsetting) process occurs. In this stage, the extrusion force increases slowly because deformation mainly takes place in the region of the billet that contacts the protruding part of the punch. Stage 2 begins when the metal starts to flow into the die cavity, marking the main forward extrusion phase. During this period, the extrusion force rises rapidly as the billet experiences a triaxial compressive stress state. In stage 3, the metal flows steadily in the direction of the punch until the desired product dimensions are achieved; the extrusion force in this phase is high and remains relatively stable.

The maximum extrusion force throughout the process is approximately 14.35 tons, indicating that the YHQ-SF150 hydraulic press fully satisfies the required forming load. In the actual forward extrusion experiments, however, the maximum force was observed to be about 20 tons, which is higher than the simulated value. This discrepancy can be attributed to practical factors not fully considered in the simulation, including variations in processing parameters, deviations in die geometry and alignment, and more complex friction conditions at the billet–die interface. These factors increase the deformation resistance during real processing. Nevertheless, the simulation still provides a reasonable estimation of the extrusion force and correctly reflects the overall trend of the extrusion process.

3.2. Effect of T6 heat treatment on the microstructure and mechanical properties of AA6061 aluminum alloy after forward extrusion

The products obtained after the forward extrusion process are shown in Figure 7a.

The dimensions of the semi-finished product meet the requirements specified in the billet design drawing (Figure 7b). This result confirms the feasibility of manufacturing component billets from AA6061 aluminum alloy using the forward extrusion method. However, as shown in Figure 7c, the defective semi-finished products exhibit incomplete filling of the die cavity and slight geometric distortion near the extruded region. These defects are mainly attributed to inconsistencies in the initial billet preparation, such as minor deviations in billet dimensions and surface condition, which lead to non-uniform material flow during extrusion. In addition, manual operation during the experimental process may have caused misalignment between the punch and the billet, resulting in localized stress concentration and asymmetric deformation. The combined effects of uneven friction conditions and non-ideal alignment hindered stable material flow, thereby preventing the billets from achieving the required shape and dimensional accuracy.

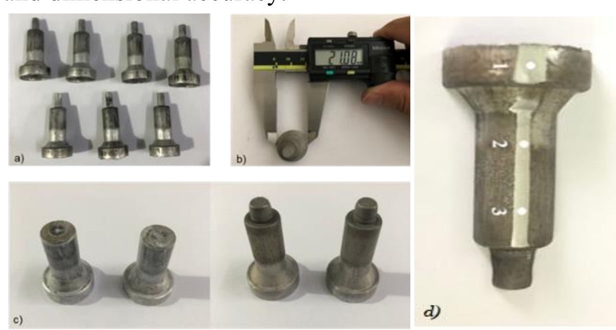

Figure 7. *Products after forward extrusion (a), dimension of the product (b), and defective product after deformation (c)*

The T6 heat treatment was carried out according to the parameters presented in Table 1. The specimens for microhardness testing (Figure 8a) and tensile testing (Figure 8b) were machined from the products obtained after the forward extrusion process. All tests were repeated at least three times for each condition to minimize experimental errors and ensure accuracy.

Figure 8. *Specimens for microhardness and tensile testing after T6 heat treatment*

3.2.1. Microstructural observation

Figure 9 shows the microstructure of the AA6061 alloy under different conditions. In the initial specimens, the material exhibits coarse and equiaxed grains with low dislocation density (Figure 9a,b). After forward extrusion, the grains become elongated along the extrusion direction and are significantly refined due to severe plastic deformation, accompanied by a marked increase in dislocation density and the formation of subgrain structures (Figure 9c,d). This high dislocation density provides favorable nucleation sites for precipitation during subsequent aging.

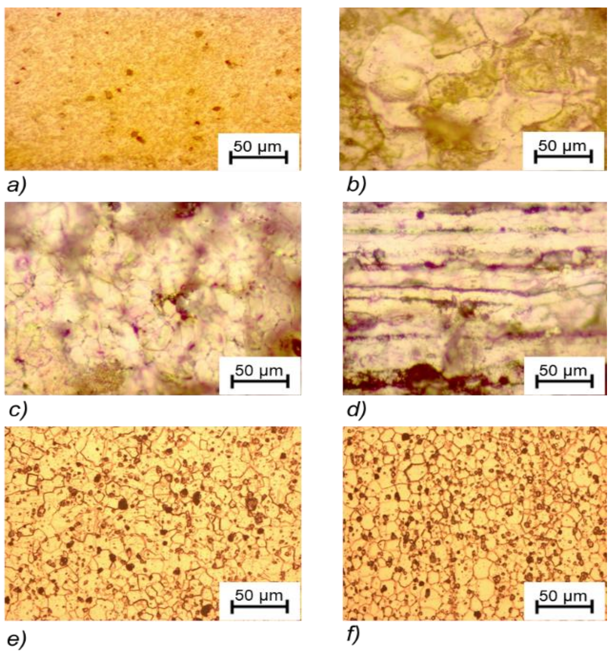

Figure 9. *Optical microscopy (OM) images of AA6061 aluminum alloy: (a, b) initial specimens, (c, d) after forward extrusion, (c) after T6 heat treatment at 175°C for 10 h, and (f) after T6 heat treatment at 175°C for 8 h*

Following T6 heat treatment, the microstructure becomes more homogeneous due to recovery and redistribution of internal defects, while fine precipitates (particularly β″) are formed and distributed within the α-Al matrix (Figure 9e,f). These coherent precipitates act as effective obstacles to dislocation motion, thereby significantly enhancing the strength and hardness of the material. With prolonged aging, the transformation of β″ into β′ and β phases may occur, leading to over-aging and a reduction in strengthening efficiency.

Pre-extrusion prior to aging not only alters the shape but also generates a high dislocation density, which serves as preferential sites for the formation of precipitates, thereby accelerating the strengthening process. Consequently, the combined effects of grain refinement induced by plastic deformation, increased dislocation density, and precipitation hardening after T6 treatment produce a synergistic strengthening effect, directly contributing to significant improvements in mechanical properties, with the UTS reaching approximately 360 MPa.

3.2.2. Microhardness test results of specimens after T6 heat treatment

The microhardness was measured at three positions, labeled 1–3, as illustrated in Figure 7d. The microhardness value used for evaluation was determined as the maximum value among the measured positions. The microhardness test results are summarized in the chart shown in Figure 10. For the experimental specimens subjected to solution treatment and artificial aging (specimens No. 3 - No. 11), the average microhardness values ranged from 95.8 HV to 109.5 HV. These values are in good agreement with the typical average microhardness of AA6061 aluminum alloy in the T6 condition (approximately 95 HV - 115 HV) [18]. For the group of specimens aged at 160°C, the microhardness increased significantly from approximately 95.8 HV (specimen No. 3) to about 104.7 HV (specimen No. 4). However, when the aging time was extended to 18 h (specimen No.5), the microhardness showed a slight decrease to around 101.4 HV. This behavior is consistent with the precipitation-hardening mechanism: in the early stage, a large number of β" phases are formed, resulting in optimal strengthening; however, with prolonged aging, these β" phases gradually transform into the more stable β' phase, thereby reducing the hardening effect [19]. For the group of specimens aged at 175°C, the microhardness exhibited higher values, with the maximum microhardness of approximately 109.5 HV obtained for specimen No. 7 after 8 h of aging. This represents the highest average microhardness among all the tested specimens, showing an increase of 52.3% compared to the average microhardness of the as-extruded specimen (specimen No. 1). However, when the aging time was extended to 10 h (specimen No. 8), the microhardness decreased. This phenomenon can be explained as follows. When the aging time was extended to 10 h at 175°C (specimen No. 8), the microhardness exhibited a decreasing trend compared to the peak value obtained at 8 h. This behavior can be attributed to the onset of the over-aging phenomenon, during which the initially formed strengthening β″ precipitates progressively transform into more stable β′ and β phases with larger sizes and lower number densities. The coarsening and reduced coherency of these precipitates diminish their effectiveness in impeding dislocation motion, leading to a reduction in microhardness and strength. This over-aging mechanism has been well documented in previous studies on Al–Mg–Si alloys, particularly AA6061, under prolonged aging at intermediate temperatures [20, 21].

For the specimens aged at 180°C, the average microhardness ranged from 99.3 HV to 107.5 HV. The microhardness increased slightly in the early stage as the aging time increased from 4 h to 6 h, but the difference was insignificant, and the values quickly reached a saturated state. At the higher aging temperature (180°C), the diffusion rates of Mg and Si atoms in the α-Al matrix are faster, leading to the rapid formation and growth of β″ phases. However, this high diffusion rate also accelerates the transformation to the more stable β′ phase, reducing the strengthening effect and causing over-aging to occur earlier [18, 21].

The microhardness measurement results indicate no significant variation in microhardness values among different measurement positions on the tested specimens. Compared with the as-received specimen (without heat treatment), the solution treatment followed by artificial aging (T6 heat treatment) significantly increased the microhardness, with a 52.3% improvement observed for the specimen aged at 175°C for 8 h.

These findings are consistent with the precipitation hardening mechanism, where microhardness increases markedly as the β″ phase predominates but decreases when this phase transforms into the coarser β′ and β phases, which are less effective in impeding dislocation motion [21]. Overall, the analysis suggests that the solution treatment followed by aging at 175°C for 8 h provides high and stable microhardness values, representing the optimal T6 heat treatment condition for AA6061 aluminum alloy within the experimental range.

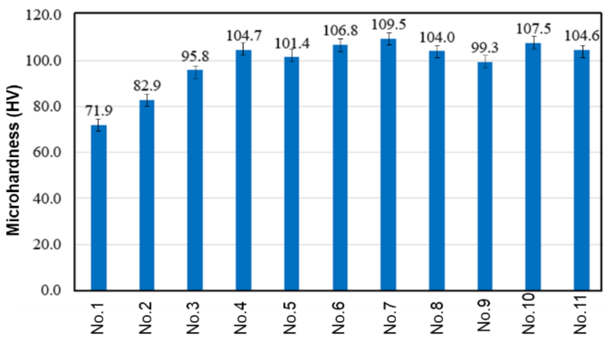

Figure 10. *Average microhardness (HV) of the experimental specimens*

3.2.3. Tensile test results of specimens after T6 heat treatment

The UTS and EL of the tensile specimens machined from the products before and after T6 heat treatment, as listed in Table 1, are presented in Figure 11.

For the group of specimens aged at 160°C, increasing the aging time from 6 h to 18 h led to an increase in UTS from 335 MPa to 367 MPa, while the EL decreased from 19.07% to 15.47%. The highest UTS of 367 MPa was obtained for the specimen aged at 160°C for 18 h, representing an increase of approximately 73% compared to the as-received specimen. This behavior is consistent with the effect of prolonged aging, where the precipitation transforms from the β″ phase to the β′ phase, resulting in higher strength but reduced ductility due to decreased uniformity and increased brittleness of the matrix [21].

For the group of specimens aged at 175°C, the UTS remained stable between 359 MPa and 362 MPa for aging times of 6 h - 10 h, while the EL ranged from 14.5% to 15.3%. Compared to the specimens aged at 160°C, the UTS showed little change; however, the required heat treatment time was significantly shorter. This indicates that at the aging temperature of 175°C, the precipitation kinetics are faster, leading to an earlier attainment of peak mechanical properties.

For the group of specimens aged at 180°C, the UTS ranged from 356 to 361 MPa, similar to that of the specimens aged at 175°C, but the EL decreased to 14.4% - 15.2%. This result reflects the early onset of over-aging due to the high atomic diffusion rate, which causes the β″ phase to rapidly transform into the coarser and sparsely distributed stable β′ and β phases. Consequently, the strengthening effect is reduced, no further improvement in mechanical properties is observed, and the material exhibits a pronounced increase in brittleness [21].

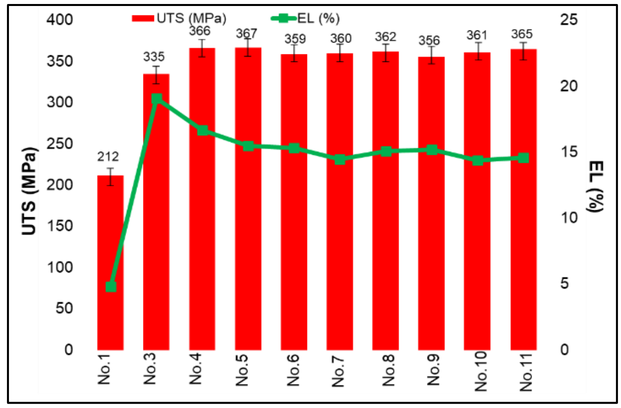

Figure 11. *Tensile test results of AA6061 aluminum alloy specimens before and after T6 heat treatment*

The results indicate that solution treatment followed by artificial aging significantly improves both UTS and EL, with UTS ranging from 335 MPa to 367 MPa and EL between 14.4% and 19.07%. Based on the analysis of the experimental results, the solution treatment followed by aging at 175°C for 8 h - 10 h can be considered the optimal heat treatment condition from a technological standpoint, as it shortens the processing time while maintaining stable mechanical properties that meet the technical requirements of the component.

4. Conclusion

The present study confirms that forward extrusion combined with T6 heat treatment is an effective thermomechanical route for enhancing the mechanical properties of AA6061 aluminum alloy. Finite element simulations successfully predicted the deformation stages and extrusion load, which were validated experimentally.

The combined process increased UTS by approximately 70% and microhardness by 52.3% compared with the annealed condition, while maintaining acceptable elongation. Aging at 175 °C for 8 h was identified as the optimal condition, offering a balanced strength–ductility response with reduced processing time.

The results demonstrate that extrusion-assisted precipitation hardening provides advantages over conventional T6 treatment and shows strong potential for manufacturing high-strength, lightweight aluminum components, suitable for lightweight structural components requiring a balance between strength and formability.

Acknowledgement: The authors would like to express their sincere gratitude to the Le Quy Don Technical University for providing laboratory facilities and technical support throughout this research.

REFERENCES

[1] Y. Sun, "The use of aluminum alloys in structures: Review and outlook", *Structures*, vol. 57, pp. 105290, 2023. https://doi.org/10.1016/j.istruc.2023.105290

[2] W. H. CoLabKhalafe, E. L. Sheng, M. R. B. Isa, and S. B. Shamsudin, "Enhancing mechanical characteristics of 6061-T6 with 5083-H111 aluminium alloy dissimilar weldments: A new pin tool design for friction stir welding (FSW*)*", *Metals*, vol. 14, no. 5, pp. 534, 2024. https://doi.org/10.3390/met14050534

[3] Z. Luo, X. Zhang, Z. Liu, H. Zhou, M. Wang, and G. Xie, "Mechanical properties and interfacial characteristics of 6061 Al alloy plates fabricated by hot-roll bonding", *International Journal of Minerals*, *Metallurgy and Materials*, vol. 31, pp. 1890-1899, 2024. https://doi.org/10.1007/s12613-023-2801-8

[4] Q. Zhao, F. Li, E. Zhu, A. F. Hashmi, and J. Niu, "Achieving excellent strength-ductility combination in AA6061 alloy via a novel thermomechanical processing technique", *Journal of Materials Science & Technology*, vol. 226, pp. 245-257, 2025. https://doi.org/10.1016/j.jmst.2024.12.016

[5] B. Bakır, H. Aljawad, F. Mert, and Ç. Karataş, "The Influence of velocity and pressure on residual stresses during the backward and forward extrusion of AA6061 T6 Aluminium Alloy", *Manufacturing Technologies and Applications*, vol. 5, no. 3, pp. 295-303, 2024. https://doi.org/10.52795/mateca.1587573

[6] M. Hawryluk *et al.*, "The application of numerical simulations to analyze the forward extrusion process along with the verification of results and tuning of the numerical model", *Computer Methods in Materials Science*, vol. 25, no. 2, pp. 27-39, 2025. https://doi.org/10.7494/cmms.2025.2.1020

[7] C. Zhang, C. Wang, Q. Zhang, G. Zhao, and L. Chen, "Influence of extrusion parameters on microstructure, texture and second-phase particles in an Al-Mg-Si alloy", *Journal of Materials Processing Technology*, vol. 270, pp. 323-334, 2019. https://doi.org/10.1016/j.jmatprotec.2019.03.014

[8] A. Deschamps, F. Livet, and Y. Bréchet, "Influence of predeformation and aging of an Al-Zn-Mg alloy-I. Microstructure evolution and mechanical properties", *Acta Materialia*, vol. 47, no. 1, pp. 281–292, 1999. https://doi.org/10.1016/S1359-6454(98)00293-6

[9] I. J. Polmear, "Precipitation hardening in aluminum alloys", *Materials Transactions*, vol. 45, no. 7, pp. 1879–1885, 2004. https://doi.org/10.2320/matertrans.45.1879

[10] C. D. Marioara, S. J. Andersen, J. Jansen, and H. W. Zandbergen, "The influence of alloy composition on precipitation in Al–Mg–Si alloys", *Metallurgical and Materials Transactions A*, vol. 32, no. 12, pp. 2615–2625, 2001. https://doi.org/10.1007/s11661-005-0185-1

[11] M. A. Ali, S. Yacob, N. I. M. Ali, M. H. A. Bakar, and V. A. Doan, "Enhanced mechanical properties of welding butt joint of aluminum alloy 6061 by T6 heat treatment process", *Journal of Advanced Manufacturing Technology*, vol. 14, no. 1, pp. 15–27, 2020.

[12] N. Kumar, S.Goel, R. Jayaganthan, and H. G. Brokmeier, "Effect of solution treatment on mechanical and corrosion behaviors of 6082-T6 Al alloy", *Metallography, Microstructure, and Analysis*, vol. 4, no. 4, pp. 411–422, 2015. https://doi.org/10.1007/s13632-015-0219-z

[13] H. Li, Z. Zheng, Z. Wu, R. Wu, and G. Liu, "Synergistic effects of extrusion and aging on precipitation and mechanical properties of 6xxx aluminum alloys", *Materials & Design*, vol. 119, pp. 90–99, 2017. https://doi.org/10.1016/j.matdes.2017.01.060

[14] Y. Wu *at el.*, "Enhanced strengthening and toughening of T6-treated 7046 aluminum alloy through severe plastic deformation", *Materials & Design*, vol. 14, no. 10, pp. 1093, 2024.

[15] S. H. Lee, H. J. Kim, J. H. Lee, and J. H. Kim, "Finite element simulation of aluminum extrusion using DEFORM-3D: prediction of extrusion load and temperature distribution", *Journal of Materials Processing Technology*, vol. 229, pp. 638–645, 2016.

[16] Y. Liu, Z. Zhao, and G. Wang, "Effect of over-aging degree on microstructures, precipitation kinetics, and mechanical properties of an ultra-high-strength Al-Zn-Mg-Cu alloy", *Coatings*, vol. 14, no. 11, pp. 1415, 2024. https://doi.org/10.3390/coatings14111415

[17] S. M. Rajaa, H. A. Abdulhadi, K. S. Jabur, and G. R. Mohammed, "Aging time effects on the mechanical properties of Al 6061-T6 alloy", *Engineering, Technology & Applied Science Research*, vol. 8, no. 4, pp. 3113-3115, 2018. https://doi.org/10.48084/etasr.2102

[18] K. Liu, F. A. Mirza, and X. G. Chen, "Effect of overaging on the cyclic deformation behavior of an AA6061 aluminum alloy", *Metals*, vol. 8, no. 7, pp. 528, 2018. https://doi.org/10.3390/met8070528

[19] Z. Cui, H. Jiang, D. Zhang, Y. Song, D. Yan, and L. Rong, "Effect of natural aging on precipitation strengthening behaviors in Al-Mg-Si alloy", *Metals*, vol. 12, no. 3, pp. 470, 2022. https://doi.org/10.3390/met12030470

[20] J. Banhart, *Age Hardening of Aluminum Alloys*, ASM Handbook: Heat Treating of Nonferrous Alloys, ASM International, 2014.

[21] R. Kahlenberg *et al.,* "On the precipitation mechanisms of β-Mg_2Si during continuous heating of AA6061," *Acta Materialia*, vol. 261, pp. 119345, 2023. https://doi.org/10.1016/j.actamat.2023.119345

[22] I. G. Flores *et al*., "Enhancing the mechanical properties of a 6061 aluminum alloy by heat treatment from the perspective of Taguchi design-of experiments", *Applied Sciences*, vol. 14, no. 3, pp. 5407, 2024. https://doi.org/10.3390/app14135407

[23] Y. K. Bin, L. Ewe, Y. W. Kean, S. R. Balasubramani, and A. W. Pramono, "Effect of heat treatment on mechanical characteristics and microstructure of aluminium alloy AA6061", *Journal of Advanced Research in Fluid Mechanics and Thermal Sciences*, vol. 124, no. 1, pp. 209-219, 2024. https://doi.org/10.37934/arfmts.124.1.209219